

L. Ye et al.: Diffusion behaviour of Pt in platinum aluminide coatings during thermal cycles

Liya Ye^a, Hongfei Chen^a, Guang Yang^a, Yuanyuan Cui^a, Hongjie Luo^a, Bin Liu^a,
Lingyi Qian^b, Yanfeng Gao^a

^aSchool of materials science and engineering, Shanghai University, Shanghai, China

^bAVIC commercial aircraft engine Co., Ltd., Shanghai, China

Diffusion behaviour of Pt in platinum aluminide coatings during thermal cycles

Two-phase PtAl₂+β-(Ni,Pt)Al and single-phase β-(Ni,Pt)Al coatings were fabricated on DD5 Ni-based superalloy and pure Ni substrates. A coating/pure Ni substrate system was studied to determine the diffusion behaviour of Pt in the Ni–Al–Pt ternary system. The evolutions of morphology, phases and component concentration during thermal cycles were analysed. It was found that there is a phase shift from PtAl₂ to β* in the two-phase coating, and Kirkendall porosity was observed in the single-phase coating. Our results further indicated that there are two different diffusion paths of Pt in the Ni–Al–Pt system.

Keywords: Platinum aluminide; Bond coat; Diffusion

1. Introduction

Thermal barrier coatings (TBCs), which are used in the hottest part of gas-turbine engines, consist of a ceramic top coat and a metallic bond coat [1, 2]. The primary function of a bond coat in TBCs is to act as a reservoir for aluminium to form a protective thermally grown oxide (TGO) [3]. For state-of-the-art TBCs, a common bond coat is Pt-modified nickel aluminide (or simply Pt aluminide) coating. At high temperatures, the diffusion behaviour of Ni, Pt, Al and substrate alloying elements are evident in the coating [4, 5]. The diffusion behaviour of Al includes outward diffusion to generate TGO and inward diffusion into the substrate. Ni diffuses outward from the substrate into the coating. Zhang et al. observed a decrease in the Pt content at the Pt-

diffused γ+γ' coating surface from 24 to 18 at.% and a Pt depth of double the original 40 μm thickness after 1 000 h at 1 000 °C [6]. Gleeson and Hayashi suggested that sufficient Pt level (>15 at.%) is necessary for uphill Al diffusion to generate TGO in the γ+γ' alloys [7, 8]. Significant loss of Pt may increase the chemical activity of Al in the γ+γ' coating so that uphill diffusion of Al becomes ineffective. Although the effect of Pt on promoting coating oxidation resistance has been confirmed by both experiments and theoretical calculations [9–12], insufficient Pt could diminish its beneficial effect [7].

Although the loss of Pt via diffusion has been recognized as a key factor of coating performance degradation, the diffusion behaviour of Pt in coatings has not been studied extensively. One reason is that the outward diffusion and interactions of substrate alloying elements in these multiple phase and multiple component systems make it a rather complex problem. One of the alloying elements is Cr, which may diffuse to the surface of the coating and generate spinel [1]. Additionally, Purvis et al. observed significant diffusion behaviour of Co, Ti and Ta in short time and significant interactions between these alloying elements [13]. Another reason is the interference of phase transformations in these complex systems. For instance, an irreversible transformation of β-(Ni,Pt)Al to γ'-Ni₃Al can occur due to the depletion of Al [14]. Since the Pt solubility limit is lower in Ni₃Al (~32 at.%) than in β-NiAl (~42 at.%) [15], Pt may precipitate out of the Ni₃Al at high temperatures and the resulting Ni₃Al has an effect on Pt diffusion.

The outward diffusion and interactions of alloying elements may interfere with the diffusion behaviour of Pt.

Building experimental models is a convenient way to simplify the multiple component systems. Models based on bulk alloys instead of coatings have been used to investigate the effect of Pt and Hf on the oxidation behaviour of coatings [9, 16]. A diffusion couple model has been used to investigate the growth mechanism of precipitates in the inter diffusion zone (IDZ) [4]. However, the bulk alloy model artificially suppresses the influence of the substrate by failing to capture inter-diffusion behaviour between the coating and substrate. Purvis et al. used pure nickel (Ni 200) as a substrate to obtain diffusion information with less interactions and noise [13]. To expand upon this, here we provide a complete coating/pure Ni substrate system diffusion model. Two-phase $\text{PtAl}_2 + \beta\text{-(Ni,Pt)Al}$ and single phase $\beta\text{-(Ni,Pt)Al}$ coatings were fabricated on pure Ni substrates. This simplifies the possible diffusion path of Pt, Ni and Al and provides fundamental diffusion data leading to insight into the degradation mechanisms of platinum aluminide bond coats. To avoid the interference of phase transformations and decrease Al depletion, the samples on pure Ni substrates were thermally cycled at a relatively low temperature.

2. Experimental procedure

The DD5 Ni-based superalloy and pure Ni substrates were provided by AVIC commercial aircraft engine Co., Ltd. (China) and Zhongnuo advanced material technology Co., Ltd., (China) respectively. The composition of DD5 is listed in Table 1. Platinum layers with different thicknesses were electroplated on the substrates using a Pt-containing electrolyte (Platinum-DNS-bath, Metakem GmbH, Germany) with a deposition rate of $2 \mu\text{m} \cdot \text{h}^{-1}$. The substrates coated with platinum layers were then aluminized. The pack powders used for aluminizing consisted of 5 wt.% Al, 0.2 wt.% NH_4Cl and 94.8 wt.% Al_2O_3 . The preparation details are listed in Table 2. Although platinum aluminide coatings are usually used at temperatures above 1100°C , the pure Ni substrates used in the present work limit the conditions for thermal cycling. Thus, the samples fabricated on pure Ni substrates were thermally cycled at a relatively low temperature of 800°C for 1 h in air and then air cooled to room temperature. The phases of the coatings before and after thermal cycling were identified by X-ray dif-

fraction (XRD) (18 KW D/MAX2500 V+/PC, Rigaku Corporation, Japan). All the samples were examined by using bulk. The surface and cross-sectional morphologies of the specimens were examined using scanning electron microscopy (SEM). The composition distribution across the coating thickness was monitored before and during thermal cycling using energy dispersive X-ray spectroscopy (EDS).

3. Results

3.1. Characterization of the as-deposited platinum aluminide coatings on DD5 Ni-based superalloy substrates

Figure 1 shows the microstructural features of the as-deposited two-phase $\text{PtAl}_2 + \beta\text{-(Ni,Pt)Al}$ and single-phase $\beta\text{-(Ni,Pt)Al}$ coatings on Ni-based superalloy substrates. Both

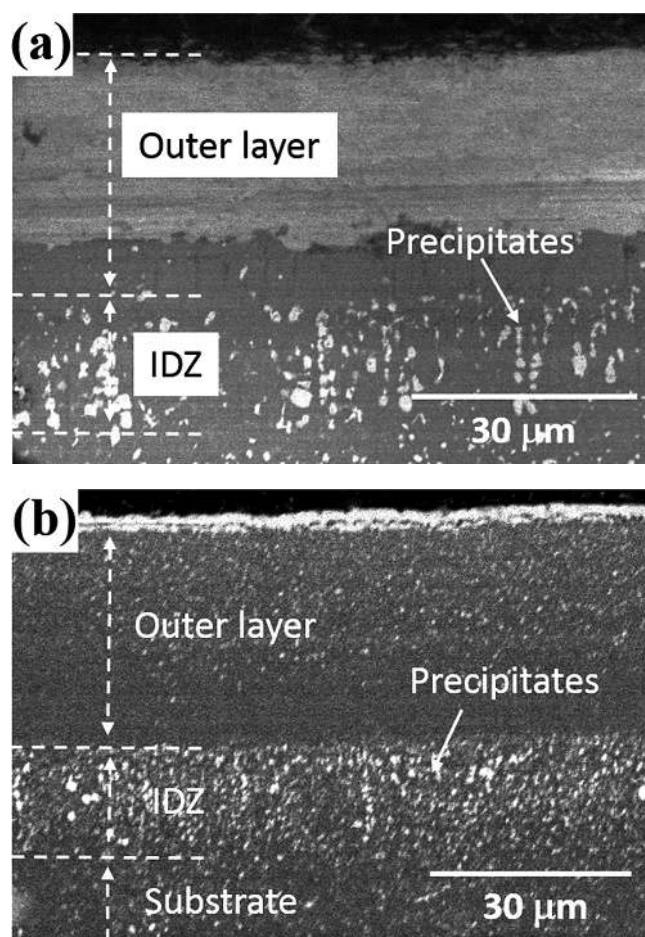


Fig. 1. Cross-sectional morphologies of the as-deposited coatings on DD5 Ni-based superalloy substrates: (a) two-phase $\text{PtAl}_2 + \beta\text{-(Ni,Pt)Al}$, and (b) single-phase $\beta\text{-(Ni,Pt)Al}$ coatings.

Table 1. Composition (wt.%) of DD5 superalloy.

Cr	Co	W	Mo	Al	Ta
4.3	9.5	7.5	1.6	5.7	6.4
Re	Hf	Nb	Zr (ppm)	C	Ni
2.1	0.09	0.7	140	0.003	Bal.

Table 2. Electroplating and aluminizing parameters.

Parameters/Sample	Electroplating time (h)	Pretreatment time (h, @ 800°C)	Aluminizing temperature ($^\circ\text{C}$)	Aluminizing time (h)
Two-phase coating	2	48	980	12
Single-phase coating	1	72	1050	12

coatings consist of an outer layer and an inter diffusion zone (IDZ) [17]. It is also seen that intermetallic precipitates (white spots) are mainly distributed in the IDZ, and some also exist in the outer layer (Fig. 1b). This is because some of the alloying elements may diffuse into the outer layer from the substrate [17, 18]. These precipitates probably interfere with the diffusion of platinum [13]. Therefore, a complete coating/pure Ni substrate system model is proposed.

3.2. Characterization of the as-deposited platinum aluminide coating/pure Ni substrate system

Figure 2a shows the microstructural features of the as-deposited two-phase $\text{PtAl}_2 + \beta\text{-(Ni,Pt)Al}$ coating on a pure Ni substrate. The outer layer has a thickness of approximately $50\text{ }\mu\text{m}$ and consists of PtAl_2 and $\beta\text{-(Ni,Pt)Al}$ phases, according to the XRD pattern (Fig. 2c). This is consistent with results reported by Tawancy [19]. Between the outer layer and the substrate lies the IDZ, which has a thickness of approximately $160\text{ }\mu\text{m}$. Because there are no alloying or refractory elements in pure Ni substrates, the IDZ does not contain any intermetallic precipitates. The $\beta\text{-(Ni,Pt)Al}$, whose XRD pattern is shown in Fig. 2d, is a nonstoichiometric single-phase which is consistent with the structure of the $\beta\text{-NiAl}$ phase (cubic; B2-type superlattice) [19].

The morphology of the as-deposited single-phase $\beta\text{-(Ni,Pt)Al}$ coating is illustrated in Fig. 2b. The depth of the Pt layer, the inner zone of which is the IDZ, is approximately $45\text{ }\mu\text{m}$. It is evident that there are voids near the interface between the outer layer and the IDZ. Such pores have also been observed in the $\beta\text{-(Ni,Pt)Al}$ coating/superalloy system after long-term oxidation [20]. There are three major fluxes in the coating. An interdiffusion of Ni and Al occurs between the coating and substrate. Al diffuses outward to supply the growth of TGO. When the diffusion fluxes of Ni and Al were not balanced and there are insufficient vacancy sinks, Kirkendall voids could form. It is possible that these voids then coalesce into large cavities because of thermal stress [5, 6].

3.3. Phases of the platinum aluminide coatings after thermal cycles

Figure 3 shows the surface morphologies and XRD patterns of the two-phase and single-phase coatings after 225 thermal cycles. After the thermal cycles, TGO forms on the surface of the coatings and the morphology is affected by some

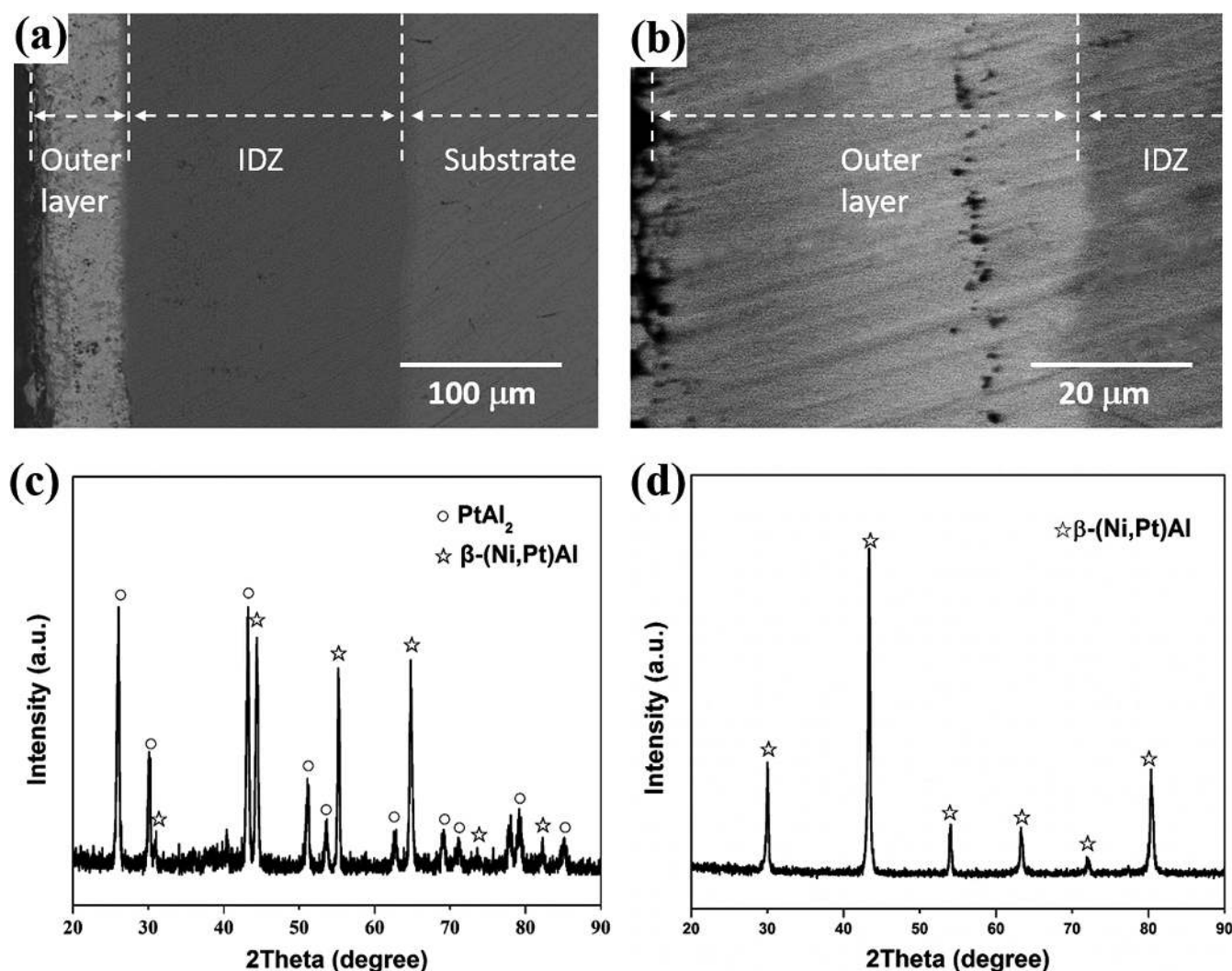


Fig. 2. Cross-sectional morphologies and XRD patterns of the as-deposited coatings in the model: (a), (c) two-phase, and (b), (d) single-phase coating.

“initial” rumpling. The surface of two-phase coating is rougher than that of the single-phase. It is seen from Fig. 3c and d that the TGO generated on the surface of both two-phase and single-phase coatings is Al_2O_3 . TGO acts as an oxygen diffusion barrier to protect the substrate from oxidation [18, 21]. From the XRD patterns, the main phases of the coatings are also detected. No Ni_3Al , which is typically generated by the depletion of Al, was observed. The results indicate that both the two-phase and single-phase coating can supply sufficient Al to generate TGO, and the diffusion behaviour of Pt in the coatings will not be affected by Ni_3Al formation.

However, there is a change of the relative intensities of the reflections for the PtAl_2 and β^* phases in the two-phase coating, as shown in Fig. 3c. In the isothermal section of the Ni–Al–Pt ternary system at 900°C (Fig. 4) [22], the area around Al_2NiPt is called the β^* superstructure, which is cubic with a lattice parameter twice that of the β -phase and is built in a similar way to PtAl_2 [23]. However, there is a difference between PtAl_2 and β^* : the 4b Wyckoff positions in PtAl_2 are vacant, while they are occupied by Ni in β^* [22, 24]. The shift from Al_2Pt to β^* observed in the XRD patterns is consistent with the gradual filling of the vacant positions by Ni.

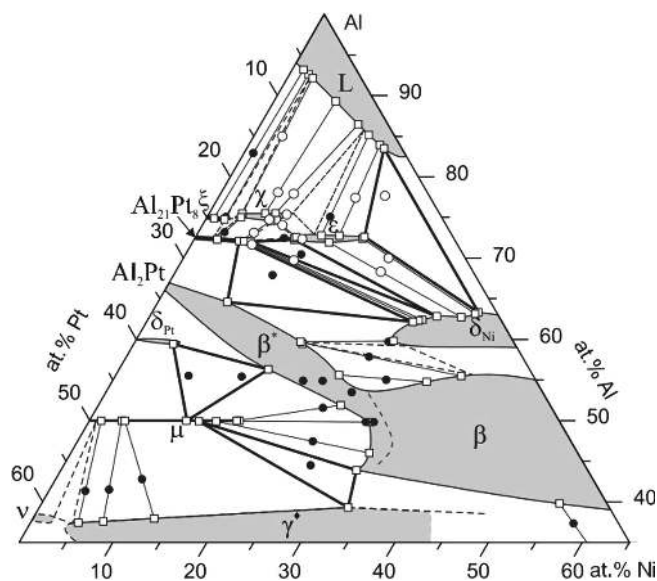


Fig. 4. The isothermal section of the Ni–Al–Pt ternary system at 900°C [22].

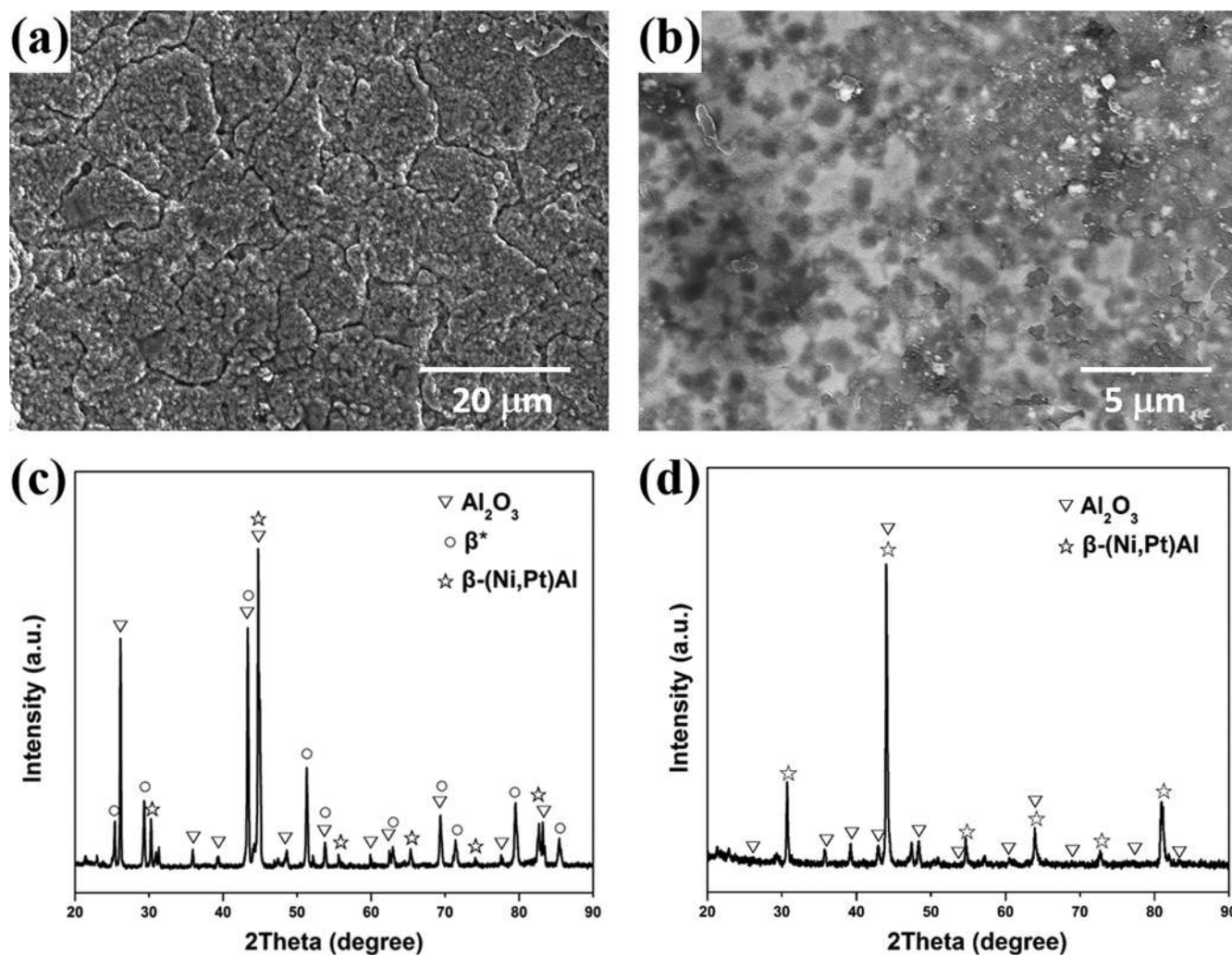


Fig. 3. Surface morphologies and XRD patterns of two types of platinum aluminide coatings after thermal cycles: (a), (c) two-phase, and (b), (d) single-phase coating.

3.4. Concentration evolution during thermal cycles

Figure 5a shows an enlarged region of the outer layer of the as-deposited two-phase coating before thermal cycling. The appearance of this region can be described as black-and-white stripes ($\sim 2 \mu\text{m}$) with a random distribution. EDS analysis (Fig. 5c) shows that the white regions are PtAl_2 -rich (higher Pt content) and the black regions are $\beta\text{-(Ni,Pt)Al}$ -rich (lower Pt content). This is consistent with a previous work, where it was observed that the increase of Pt layer thickness favoured the formation of PtAl_2 phase in the fabrication process [25]. After thermal cycling, some PtAl_2 -rich white stripes grew larger ($\sim 10 \mu\text{m}$, Fig. 5b). The composition changed from $\text{Al}_{60}\text{Ni}_{15}\text{Pt}_{35}$ to $\text{Al}_{60}\text{Ni}_{20}\text{Pt}_{20}$, which is attributed to the diffusion of Ni from Ni-rich $\beta\text{-(Ni,Pt)Al}$ into the vacant 4b Wyckoff positions of PtAl_2 , leading to a phase change from PtAl_2 to β^* .

Comparing Fig. 5c with Fig. 5d, the Al content remains constant ($55 \sim 65 \text{ at.}\%$) across the depth of the outer layer, while the Pt and Ni contents changed oppositely. Especially in the range of $0 \sim 20 \mu\text{m}$, the Pt content decreased in some regions, where the composition changed from $\text{Al}_{60}\text{Ni}_{15}\text{Pt}_{35}$ to $\text{Al}_{60}\text{Ni}_{35}\text{Pt}_5$. This is a result of the interdiffusion behaviour between the Pt and Ni. Both Jang and Marino have re-

ported that Pt will always preferentially substitute for Ni in the sublattice [26, 27]. Grushko et al. suggested that the β -phase structure is more stable than β^* [22]. Therefore, it is concluded that Pt diffused from PtAl_2 to $\beta\text{-(Ni,Pt)Al}$ by way of the Ni sublattice in the two-phase coating.

Figure 6 shows the partially-enlarged details and concentration evolution of the single-phase coating before and after thermal cycling. It is seen that the number of voids near the interface of outer layer and IDZ increased and that some voids coalesced into large cavities (Fig. 6b). As shown in Fig. 6c and d, the content of Al remains approximately 40 at.% across the depth of the outer layer during thermal cycles. The Ni content is significantly higher overall after thermal cycling and also increases with increasing depth from the surface. This is caused by outward diffusion of Ni from the substrate into the coating. The Pt content varies between $0 \sim 5 \text{ at.}\%$ and decreases with increasing depth from the surface. It is therefore inferred that Pt diffuses in the same direction as Ni by way of the Ni sublattice.

Because the average Ni content in the outer layer is lower in the two-phase coating (20 at.%) than in the single-phase coating (60 at.%), the concentration gradient of Ni between the substrate and the outer layer is higher in the two-phase coating than in the single-phase coating. As a result,

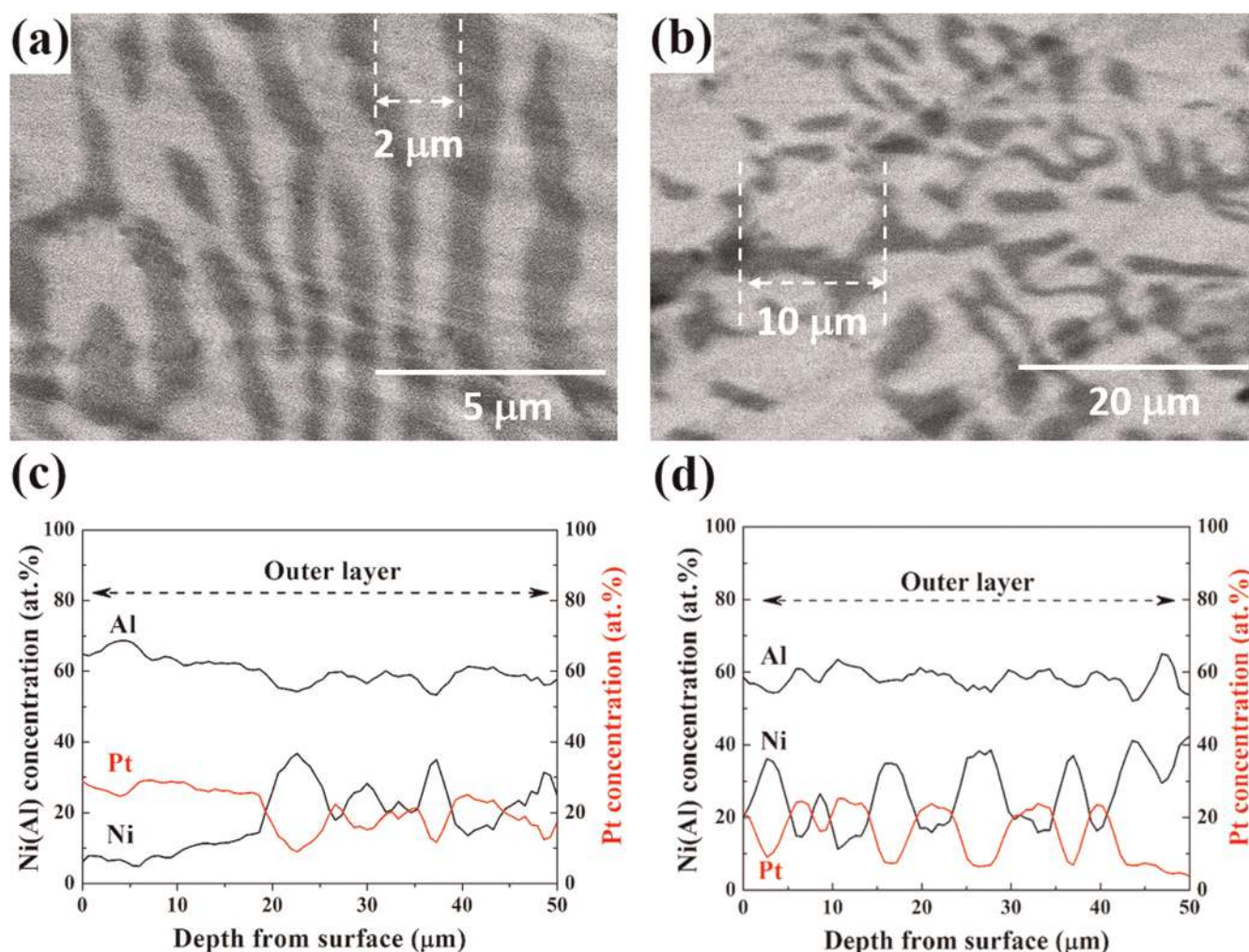


Fig. 5. Partially-enlarged details and concentration profiles of Pt, Ni and Al across the outer layer of the two-phase coating: (a), (c) before, and (b), (d) after thermal cycling.

plenty of Ni diffused from the substrate to the outer layer in the two-phase coating. Diffusion of Ni in NiAl is via vacancy diffusion because the large size of Ni prevents its interstitial movement. First-principle calculations show that the preference of Pt for the Ni sublattice could promote the formation of Ni vacancies [26]. Therefore, the interdiffusion of Pt and Ni is active in the two-phase coating. However, in the single-phase coating, the magnitude of Ni diffusion into the outer layer is less than in the two-phase coating. Although the interdiffusion of Pt and Ni is weaker than that in the two-phase coating, there is a slight diffusion of Pt towards the surface. The Pt–Al bond is stronger than the Ni–Al bond, based on calculations from Knudsen-cell chemical activity measurements [28]. In addition, the PtAl compound has the most negative formation enthalpy among PtAl, NiAl and NiPt stoichiometric B2 compounds, calculated by the statistical-mechanical Wagner–Schottky model [27]. Both of them are energetically favourable to form nearest-neighbour Pt–Al bonds. Therefore, the diffusion of Pt from inside to outside in the single-phase coating is forced by maximizing the number of nearest-neighbour Pt–Al bonds.

4. Discussion

In the two-phase coating, there is a composition shift from PtAl₂ to β^* and the interdiffusion of Pt and Ni is active. Ni diffused from Ni-rich β -(Ni,Pt)Al into the vacant 4b Wyckoff positions of PtAl₂ and Pt diffused from PtAl₂ to β -(Ni,Pt)Al by way of the Ni sublattice. Audigié et al. observed a phase transformation from α -NiPtAl to γ -(Ni,Pt,Al) due to component diffusion at 1100 °C for 1 h [29]. During 225 thermal cycles, the Al content remains constant. Zhang et al. also observed that the Al content only minimally changed in the Pt-diffused $\gamma+\gamma'$ coatings after 1000 h at 900 °C [6]. Figure 5c and d present the concentration evolution of the two-phase coating before and after thermal cycles, respectively. These plots confirm that the Al concentration keep constant at approximately 60 at.%, while the Ni and Pt concentrations changed as a result of thermal cycles. This highlights that Pt diffuses by way of the Ni sublattice. In the single-phase coating, the Al concentration keeps constant at approximately 40 at.% during thermal cycles. This also confirms that Pt diffuses by way of the Ni sublattice. Forced by maximizing the number of

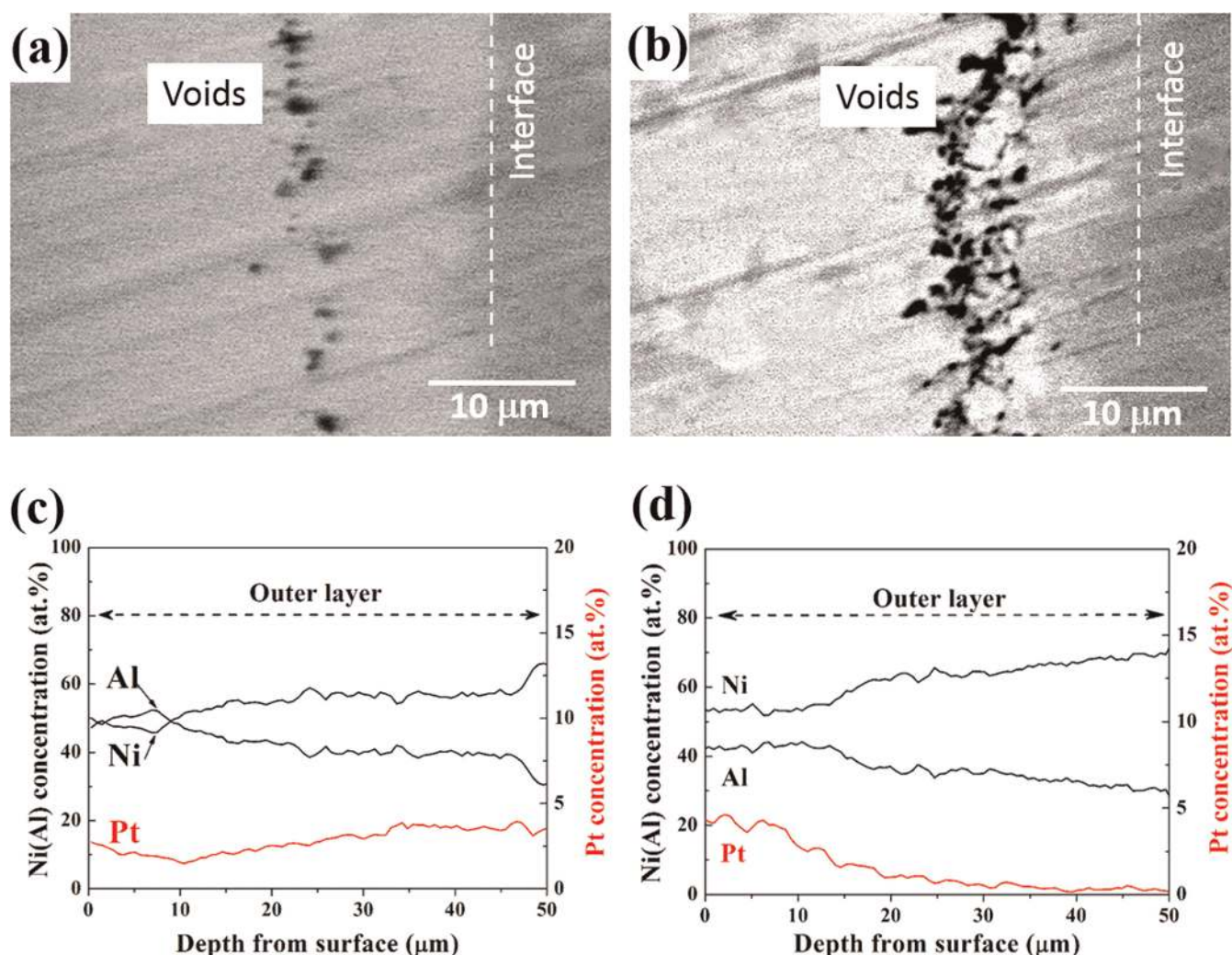


Fig. 6. Partially-enlarged details and concentration profiles of Pt, Ni and Al across the outer layer of the single-phase coating: (a), (c) before, and (b), (d) after thermal cycling.

nearest-neighbour Pt-Al bonds, Pt diffused from inside to outside by the way of the Ni sublattice.

In the as-fabricated single-phase coating, a number of voids were observed near the outer layer/IDZ interface. Such voids have also been observed as Kirkendall porosity in Pt-plated pure Ni after 2 h at 950 °C [13]. Haynes et al. suggested that the voids result from uphill diffusion of Al towards the surface [30]. After thermal cycling, the concentration gradients of Ni and Pt were of opposite sign. The outward flux of Pt and Al near the interface between the outer layer and IDZ was not balanced by the flux of Ni from the substrate. Thus, the voids near the outer layer/IDZ interface coalesced into large cavities. First, Pt decreases the Al activity, which promotes the uphill diffusion of Al to the surface [8]. Second, the diffusion of Ni from the substrate to the outer layer is weak and the replenishment of Ni is not sufficient. Audigé et al. suggested that the void location corresponds to the Al depletion zone (or the Pt diffusion front) [29]. However, no voids were observed in the two-phase coating. The average Al content in the outer layer of the two-phase coating is 20% higher than that of the single-phase coating. Thus, the absence of voids in the two-phase coating could be due to having more Al to deplete and to strong outward diffusion of Ni, forced by a higher concentration gradient than that of the single-phase coating. Still, voids may occur after more thermal cycles.

5. Conclusions

In this work, two-phase $\text{PtAl}_2 + \beta\text{-(Ni,Pt)Al}$ and single-phase $\beta\text{-(Ni,Pt)Al}$ coatings were fabricated on Ni-based superalloys and pure Ni substrates, respectively. In the coating/pure Ni substrate system, coatings exhibit protectiveness as bond coats in TBCs.

In the two-phase coating, there is a phase shift from PtAl_2 to β^* . Ni diffused from Ni-rich $\beta\text{-(Ni,Pt)Al}$ into the vacant 4b Wyckoff positions of PtAl_2 and Pt diffused from PtAl_2 to $\beta\text{-(Ni,Pt)Al}$ by way of the Ni sublattice. In the single-phase coating, forced by maximizing the number of nearest-neighbour Pt-Al bonds, Pt diffused from inside to outside by way of the Ni sublattice, and Kirkendall porosity was observed.

The authors acknowledge the financial support by Shanghai Outstanding Technical Leaders Plan of Shanghai Municipal Science and Technology Committee (14XD1424000) and National Natural Science Foundation of China (51402183, 51602187, and 51602188).

References

- [1] D.R. Clarke, M. Oechsner, N.P. Padture: *MRS Bull.* 37 (2012) 891. DOI:10.1557/mrs.2012.232
- [2] M. Bacos, J. Dorvaux, S. Landais, O. Lavigne, R. Mévrel, M. Poulain, C. Rio, M. Vidal-Sétif: *The ONERA Journal* 3 (2011) 1.
- [3] T.M. Pollock, D.M. Lipkin, K.J. Hemker: *MRS Bull.* 37 (2012) 923. DOI:10.1557/mrs.2012.238
- [4] P. Kiruthika, S.K. Makineni, C. Srivastava, K. Chattopadhyay, A. Paul: *Acta Mater.* 105 (2016) 438. DOI:10.1016/j.actamat.2015.12.014
- [5] V.K. Tolpygo, D.R. Clarke: *Acta Mater.* 48 (2000) 3283. DOI:10.1016/S1359-6454(00)00156-7
- [6] Y. Zhang, J.P. Stacy, B.A. Pint, J.A. Haynes, B.T. Hazel, B.A. Nagaraj: *Surf. Coat. Tech.* 203 (2008) 417. DOI:10.1016/j.surfcoat.2008.08.053
- [7] B. Gleeson, W. Wang, S. Hayashi, D.J. Sordelet: *Mater. Sci. Forum* 461 (2004) 213. DOI:10.4028/www.scientific.net/MSF.461-464.213

- [8] H. Shigenari, W. Wen, J.S. Daniel, G. Brian: *Metall. Mater. Trans. A* 36 (2005) 1769. DOI:10.1007/s11661-005-0041-3
- [9] Y. Chen, X. Zhao, M. Bai, A. Chandio, R. Wu, P. Xiao: *Acta Mater.* 86 (2015) 319. DOI:10.1016/j.actamat.2014.12.023
- [10] Z. Xu, Z. Wang, G. Huang, R. Mu, L. He: *J. Alloys Compd.* 637 (2015) 226. DOI:10.1016/j.jallcom.2015.02.177
- [11] C. Liguio, A.M. Limarga, D.R. Clarke: *Comp. Mater. Sci.* 50 (2010) 77. DOI:10.1016/j.commatsci.2010.07.009
- [12] D.S. Balint, J.W. Hutchinson: *J. Mech. Phys. Solids* 53 (2005) 949. DOI:10.1016/j.jmps.2004.11.002
- [13] A.L. Purvis, B.M. Warnes: *Surf. Coat. Tech.* 133 (2000) 23. DOI:10.1016/S0257-8972(00)00890-2
- [14] V.K. Tolpygo, D.R. Clarke: *Surf. Coat. Tech.* 203 (2009) 3278. DOI:10.1016/j.surfcoat.2009.04.016
- [15] S. Hayashi, S.I. Ford, D.J. Young, D.J. Sordelet, M.F. Besser, B. Gleeson: *Acta Mater.* 53 (2005) 3319. DOI:10.1016/j.actamat.2005.03.046
- [16] V.K. Tolpygo, K.S. Murphy, D.R. Clarke: *Acta Mater.* 56 (2008) 489. DOI:10.1016/j.actamat.2007.10.006
- [17] D.K. Das: *Prog. Mater. Sci.* 58 (2013) 151. DOI:10.1016/j.pmatsci.2012.08.002
- [18] H.M. Tawancy, L.M. Al-Hadrami: *J. Eng. Gas Turb. Power* 134 (2012) 1. DOI:10.1115/1.4004131
- [19] H.M. Tawancy: *Oxid. Met.* 81 (2014) 237. DOI:10.1007/s11085-013-9454-3
- [20] N. Vialas, D. Monceau: *Surf. Coat. Tech.* 201 (2006) 3846. DOI:10.1016/j.surfcoat.2006.07.246
- [21] R.W. Jackson, D.M. Lipkin, T.M. Pollock: *Acta Mater.* 80 (2014) 39. DOI:10.1016/j.actamat.2014.07.033
- [22] B. Grushko, D. Kapush: *J. Alloys Compd.* 594 (2014) 127–132. DOI:10.1016/j.jallcom.2014.01.114
- [23] B. Grushko: *J. Alloys Compd.* 541 (2012) 88–93. DOI:10.1016/j.jallcom.2012.06.114
- [24] B. Grushko, D. Kapush, V. Konoval, V. Shemet: *Powder Metallurgy and Metal Ceramics* 50 (2011) 462–470. DOI:10.1007/s11106-011-9350-9
- [25] M.Z. Alam, S.V. Kamat, V. Jayaram, D.K. Das: *Acta Mater.* 67 (2014) 278. DOI:10.1016/j.actamat.2013.12.033
- [26] K. Marino, E. Carter: *Acta Mater.* 56 (2008) 3502. DOI:10.1016/j.actamat.2008.03.029
- [27] C. Jiang, M.F. Besser, D.J. Sordelet, B. Gleeson: *Acta Mater.* 53 (2005) 2101. DOI:10.1016/j.actamat.2004.12.038
- [28] E. Copland: *Technical Report No. NASA/CR-2005-213330* (NASA, 2005), 2005.
- [29] P. Audigé, A.R.V. Put, A. Malie, P. Bilhe, S. Hamadi, D. Monceau: *Surf. Coat. Tech.* 260 (2014) 9. DOI:10.1016/j.surfcoat.2014.08.083
- [30] J.A. Haynes, B.A. Pint, Y. Zhang, I.G. Wright: *Surf. Coat. Tech.* 204 (2009) 816. DOI:10.1016/j.surfcoat.2009.09.071

(Received March 3, 2017; accepted August 8, 2017; online since November 2, 2017)

Correspondence address

Dr./Prof. Yanfeng Gao
School of Materials Science and Engineering
Shanghai University
99 Shangda road
Shanghai, 200444
P.R. China
Tel.: +086-021-66138005
E-mail: yfgao@shu.edu.cn

Bibliography

DOI 10.3139/146.111572
Int. J. Mater. Res. (formerly Z. Metallkd.)
109 (2018) 1; page 3–9
© Carl Hanser Verlag GmbH & Co. KG
ISSN 1862-5282